Journal of Crystal Growth 96 (1989) 27–39
North-Holland, Amsterdam

ORIENTATION DEPENDENT AMPHOTERIC BEHAVIOR OF GROUP IV IMPURITIES IN THE MOLECULAR BEAM EPITAXIAL AND VAPOR PHASE EPITAXIAL GROWTH OF GaAs

B. LEE, S.S. BOSE, M.H. KIM, A.D. REED and G.E. STILLMAN

Center for Compound Semiconductor Microelectronics, Coordinated Science Laboratory and Materials Research Laboratory, University of Illinois at Urbana - Campaign, Urbana, Illinois 61801, USA

W.I. WANG * and L. VINA

IBM Thomas J. Watson Research Center, P.O. Box 218, Yorktown Heights, New York 10598, USA

and

P.C. COLTER **

Universal Energy Systems, Inc., Dayton, Ohio 45432, USA

Received 23 September 1988; manuscript received in final form 21 November 1988

The incorporation and amphoteric behavior of the Group IV impurities, Si, Ge, and C, have been investigated in molecular beam epitaxial (MBE) and $AsCl_3$ vapor phase epitaxial (VPE) GaAs samples grown on (100), (211) and (311) substrates. Spectroscopic analysis using photothermal ionization spectroscopy and photoluminescence combined with variable temperature Hall effect measurements indicate that the amphoteric behavior of the Group IV impurities is kinetically influenced by different surface reaction processes associated with the substrate orientation. A description of the kinetic growth process has been developed which considers the bonding structure of the growth surface and the related surface reaction mechanisms of Group III, IV, and V sources in MBE and VPE growth. With these kinetically limited growth processes the experimentally observed impurity incorporation results can be explained based on the different reaction behavior associated with the surface bonding of the different adsorbed chemical species on the dynamic growth front.

1. Introduction

Among the Group IV elements, Si and Ge are the only truly amphoteric shallow impurities in GaAs. It has been shown that Si incorporates primarily as a donor in VPE, MOCVD, and MBE layers grown on (100) oriented substrates, and primarily as an acceptor in LPE (100) layers [1]. Ge incorporates only as an acceptor in LPE (100) layers for ordinary growth temperatures [2] but is incorporated primarily as a donor in VPE and MOCVD layers grown on (100) substrates [1]. Ge doped MBE (100) layers can be either n- or p-type depending on the V/III ratio and the substrate temperature [3,4]. In contrast with early speculation [5], C has never been observed as a donor in photothermal ionization spectroscopy [6] or in local mode infrared absorption measurements [7], but it is commonly observed to be the dominant residual acceptor for all growth techniques except $AsCl_3$-VPE. Although Sn is an amphoteric impurity and a commonly used n-type dopant in LPE and VPE, Sn creates only a deep acceptor level [8]. Pb is the least studied Group IV element in GaAs, but there is no conclusive evidence that Pb is incorporated as a substitutional impurity in GaAs [9–11].

* Present address: Department of Electrical Engineering, Columbia University, New York, New York 10027, USA.
** Present address: EMCORE Co., Somerset, New Jersey 08873, USA.

0022-0248/89/$03.50

Epitaxial growth on substrates with polar surface orientations, (h11)A and (h11)B, where $h = 1, 2, 3, \ldots, n$ has been investigated in order to understand the growth mechanisms [12] and the incorporation and amphoteric behavior of individual impurity species [13]. Effects of these different orientations on impurity behavior have been observed in LPE [14], VPE [15,16], MOCVD [17], and MBE GaAs layers [18]. Both the (211) and the (311) orientations which Sangster [19] suggested to be ideal for III–V epitaxy, have produced particularly interesting results for GaAs epitaxial growth. The amphoteric behavior of Si and residual C impurities in lightly Si doped MBE GaAs layers grown simultaneously on (100), (311)A, and (311)B oriented substrates has been previously studied [20]. From spectroscopic and Hall effect analyses of those samples, it was found that for an n-type (100) layer the Si amphoteric ratio, defined as the ratio of the concentration of Si acceptors to the concentration of Si donors, $[Si_{As}]/[Si_{Ga}]$, was 0.08. A (311)B layer grown simultaneously was also n-type, but the Si amphoteric ratio was 0.01, and it was estimated that the total Si impurity concentration ($[Si] = [Si_{Ga}] + [Si_{As}]$) was reduced from that of the (100) layer by 20%. In addition, the C acceptor concentration, $[C_{As}]$, in this same (311)B layer, was also reduced by approximately 20% compared to the $[C_{As}]$ in the (100) grown layer. A sample grown on a (311)A oriented substrate was relatively uncompensated p-type due to Si incorporation primarily as an acceptor, with the Si amphoteric ratio greater than 4. However, in contrast to the behavior of Si in this (311)A grown layer where $[Si_{As}]$ was increased, the $[C_{As}]$ was further reduced so that $[C_{As}]$ was only about 7% of that in the (100) layer. These results show that the incorporation behavior of Group IV impurities is not only strongly influenced by the growth orientation but is also dependent on the individual impurity species.

In the following two sections we present additional experimental results on residual impurity incorporation in *undoped* n-type MBE and $AsCl_3$-VPE epitaxial GaAs and summarize the amphoteric behavior of the Group IV impurities. In section 4 we describe the kinetic model of the orientation dependence of impurity incorporation in GaAs that is consistent with all of the experimental results.

2. Experimental

Even though undoped MBE GaAs layers grown on (100) oriented substrates are normally p-type because the residual $[C_{As}]$ is greater than N_D, recent results on undoped layers grown on (311)B oriented substrates have shown these layers to be high purity n-type due to the suppression of the C incorporation on the (311)B polar substrates as described above. In this section we present new experimental results on an undoped n-type MBE GaAs layer, sample 828(311)B, which was grown on a (311)B oriented substrate using a solid As source. This sample was very high purity n-type, while samples grown on (100) oriented substrates under the same growth conditions are always p-type with hole concentrations in the 10^{14}–10^{15} cm^{-3} range. The growth temperature was about 590°C, and the growth rates for both samples grown on (311)B and (100) oriented substrates were equal at 1.5 $\mu m/h$, which is consistent with observations that MBE growth rates depend only on the Ga beam flux. The equivalent beam partial pressure ratio of As_4/Ga was 15–20 in the As stabilized condition. The samples were grown on Cr doped semi-insulating substrates. The substrates were etched with 7 : 1 : 1 ($H_2SO_4 : H_2O_2 : H_2O$) and rinsed with deionized water before loading into the growth chamber. The as-grown surfaces for both samples were smooth.

Sample 133B which was grown on a (211)A oriented semi-insulating substrate using the $Ga–AsCl_3–H_2$ growth technique was also studied. Since it has been known that undoped n-type $AsCl_3$-VPE layers grown on (211)A and (311)A orientations are higher purity and less compensated than those grown on the (100) orientation [15], it is interesting to compare the differences in the impurity incorporation behavior between VPE and MBE GaAs growth on (211)A surfaces. The detailed growth conditions for this undoped $AsCl_3$-VPE sample are described elsewhere [21]. The surface morphology of sample 133B was mirror-like.

3. Results

The n-type MBE and VPE GaAs samples in table 1 were characterized using variable temperature Hall effect measurements, photothermal ionization spectroscopy (PTIS), and photoluminescence (PL) techniques, which have been described elsewhere [9]. Table 1 shows the carrier concentration and Hall mobility at 77 K, and the total donor and acceptor concentrations, N_D and N_A determined from variable temperature (4.2–300 K) Hall effect measurements. The Hall effect results in table 1 indicate that the $AsCl_3$-VPE (chloride) sample is relatively uncompensated compared to most GaAs materials with $N_A/N_D = 0.09$, and that the MBE sample grown on the (311)B oriented substrate (sample 828(311)B) with $N_D - N_A = 8 \times 10^{13}$ cm^{-3} is one of the highest purity MBE GaAs samples that has been grown thus far.

Fig. 1 shows the photothermal ionization spectra of 1s–2p ($m = -1$) transitions for both n-type samples in table 1. The dominant residual donor species in the $AsCl_3$-VPE sample is Si, with smaller concentrations of S, Ge, and either Se or Sn which cannot be distinguished spectroscopically because of their nearly identical central call shifts. Because of absorption saturation effects [22], the Si peak for sample 133B is anomalously broad compared with the S and Ge peaks, indicating that the relative donor concentrations for this sample are no longer proportional to the relative amplitudes of the peaks due to different donor impurity species. In this case, the relative concentrations are more closely related to the relative FWHMs of the individual donor peaks. Analysis of these data, considering the FWHMs of the donor peaks, suggests that Si accounts for at least 80% of N_D in sample 133B. From the spectrum for sample 828(311)B, the dominant residual donor species is S, with trace levels of Si, either Se or Sn, and Ge.

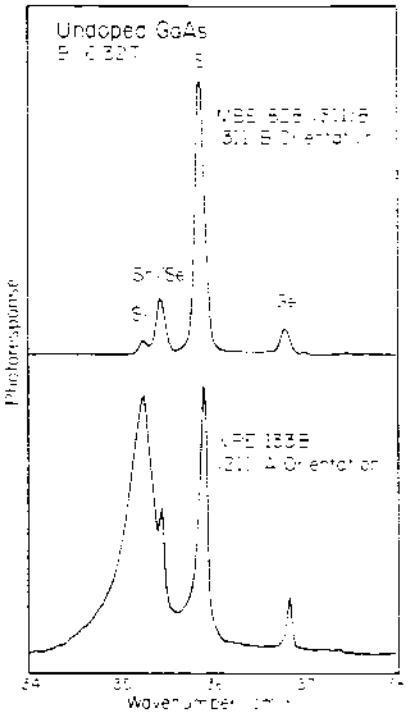

Fig. 1. Photothermal ionization spectra of 1s-2p ($m = -1$) transitions for two undoped n-type GaAs samples grown on a (311)B GaAs substrate by MBE technique and a (211)A substrate by VPE technique.

Since the FWHMs for all the donor peaks in this spectrum are nearly equal, the relative concentrations of the donor species can be accurately determined from the relative amplitudes of the corresponding donor peaks.

Fig. 2 shows the PL spectra of conduction band-to-acceptor and donor-to-acceptor transitions taken at 1.7 K with low excitation intensity using an Ar^+ laser for the same two samples. From the relative peak intensity of the neutral donor-to-acceptor peaks (D°–A°), the dominant residual acceptor species in the (211)A $AsCl_3$-VPE sample is Zn, with relatively low concentrations of

Table 1
Growth orientations and Hall effect measurements

Sample	Orientation	μ_{77} (cm^2/V·s)	n_{77} (10^{14} cm^{-3})	N_D (10^{14} cm^{-3})	N_A (10^{14} cm^{-3})
MBE 828(311)B	(311)B	180,000	0.1	0.5	0.2
VPE 133B	(211)A	168,000	1.13	1.92	0.17

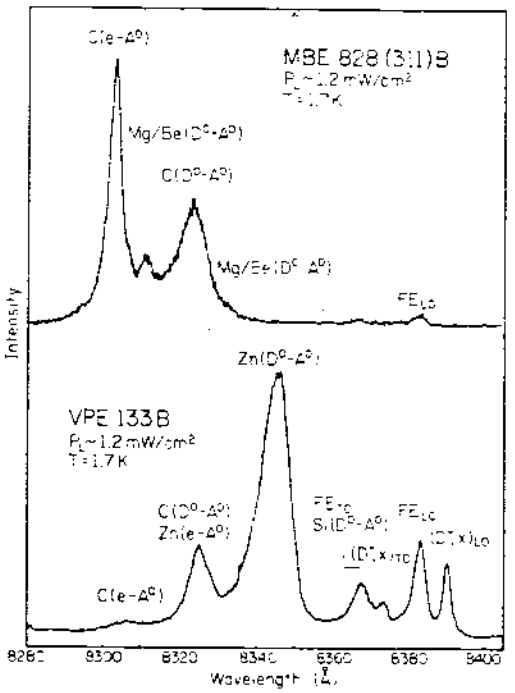

Fig. 2. PL spectra of (D^0-A^0) and $(e-A^0)$ transitions, recorded at 1.7 K and low excitation level for two undoped n-type GaAs samples.

C and Si acceptors. Zn is commonly found to be the dominant acceptor species in chloride samples grown on (100) substrates, but the Zn acceptor concentration is substantially lower in this sample, presumably due to a long bakeout of the Ga source [21]. The dominant residual acceptor species in the MBE sample 828(311)B is C, with a concentration of 2.0×10^{13} cm^{-3}. The extremely low C concentration in this layer is attributed to the orientation dependent incorporation effect described above [20].

From the relative concentrations of individual donor and acceptor impurity species determined from the relative amplitudes of the corresponding peaks in PTIS and PL spectra, and N_D and N_A determined from the variable temperature Hall effect measurements, the absolute concentration of individual donor and acceptor species can be estimated. The Si amphoteric ratio in this (211)A chloride sample is about 0.01, which is much smaller than the Si amphoteric ratio of 0.1 in chloride samples grown on (100) substrates studied previously [23]. The fact that Si is observed to be the dominant donor in sample 133B is consistent with DiLorenzo's results [15] which show that Si is an important residual impurity species, incorporating primarily as a donor in $AsCl_3$-VPE GaAs layers grown on both (211)A and (311)A oriented substrates. Although Si incorporates primarily as a donor in both VPE and MBE grown GaAs (100) layers, the amphoteric behavior of Si is evidently different for the (311)A layers grown by the VPE and MBE techniques, since Si is incorporated preferentially as a donor in VPE (311)A grown layers, and yet it is preferentially incorporated as an acceptor in MBE (311)A grown layers.

In sample 828(311)B, the residual Si is obviously incorporated primarily as a donor since $[Si_{As}]$ is below the detection limit in the PL spectrum of fig. 2. The dominant residual donor species in this MBE sample is S, but the S donor concentration $[(S_{As}])$ is lower than that in the other (100) MBE layers we have studied previously [20]. Although increased purity of the solid As source material could be partly responsible for the reduction of $[S_{As}]$, it is probably that the small S concentration of 4×10^{13} cm^{-3} in sample 828(311)B is partly due to an orientation dependent S reduction similar to that observed for C, resulting in the growth of this very high purity n-type MBE GaAs.

4. Kinetic model of amphoteric impurity incorporation

The amphoteric incorporation behavior of Si and Ge on (100) oriented substrates has been previously studied by the theoretical treatments of Teramoto in LPE growth [24], and extensive studies in VPE growth [11,25] and MBE growth [3,26]. The theoretical amphoteric behavior under the different epitaxial growth techniques is based on equilibrium thermodynamic treatments. Qualitatively, it was speculated that the strong preference of the amphoteric impurities for the Ga site in VPE and MBE as compared to LPE was due to the large value of the As activity in the former growth environments, which leads to a larger Ga vacancy concentration in the solid GaAs and, hence, enhanced incorporation of impurities on Ga sites [1]. However, equilibrium thermodynamic

considerations alone based on this site vacancy model discussed above cannot explain the orientation dependence of the amphoteric behavior of Si in $AsCl_3$-VPE and MBE growth in general. It is impossible to explain using equilibrium thermodynamics, for example, the contrast in amphoteric behavior of Si between $AsCl_3$-VPE and MBE for growth on the same polar surface, either (211)A or (311)A, or the fact that Si is preferentially a donor in both $AsCl_3$-VPE and MBE (100) grown layers. Neither can equilibrium thermodynamics explain the contrast in behavior C and Si acceptor incorporation where $[Si_{As}]_{(311)A} \gg [Si_{As}]_{(311)B}$ but $[C_{As}]_{(311)A} \ll [C_{As}]_{(311)B}$. Our spectroscopic results strongly suggest that surface kinetic reactions during epitaxial growth play the dominant role in the amphoteric behavior of Group IV impurities rather than simple site availability.

4.1. Surface bonding geometry

To understand the orientation dependent amphoteric behavior of Group IV impurities, it is necessary to consider the surface bonding geometry of the different orientations. Fig. 3 shows the surface geometry relationships between (111)A or (111)Ga, and (100) surfaces for the zinc blende crystal structure using the two-fold coordinated configuration [27]. Although this is a simplified, two-dimensional drawing of the crystal structure,

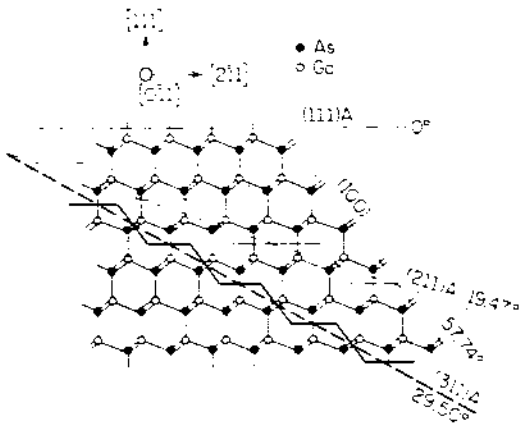

Fig. 3. The surface geometry relationships between (111)A and (100) surfaces for the zinc blende crystal structure using the two-fold coordinated configuration.

the theoretical surface bond energy is reasonably close to that of the real three-dimensional crystal structure [28]. The surface structure of the (211)A and (311)A planes are very similar, with components of both the (100) and (111)A bonding geometries. The microscopic surface structure of these (211)A and (311)A planes can be considered to be composed to periodic steps similar to those observed on MBE Si surfaces grown on substrates misoriented a few degrees from (111) [29]. As shown in the figure, the (211)A close packed surface is composed of periodic steps with one (100) step edge atom and two (111)A terrace atoms, while the (311)A surface is composed of equal numbers of (100) step edge and (111)A terrace atoms. The (311)A surface has a sequence of pairs consisting of an As surface atom with two dangling bonds, as for the (100) configuration (analogous to the zigzag periodic bond chain (PBC) in the $[01\bar{1}]$ direction [30]), and a Ga surface atom with one dangling bond, as for the (111)A configuration. The (311)B surface has Ga and As atomic bond configurations identical to those of the (311)A surface with the Ga and As atoms interchanged.

The atomic geometry of the covalent bond structure in a crystal represents a configuration which minimizes the total energy of the dangling bonds at the crystal surface [31]. In addition, due to charge neutrality, the polar nature of the zinc blende structure requires that the polar surface after termination of epitaxial growth should be identical to the substrate polar surface. Thus, an equal number of Ga and As atoms should be bonded in the grown crystal for any polar surface orientation growth. During the MBE growth of (311)A layers in the As stabilized condition, Ga atoms can bond independently at the sites along any (100) step edge with no net change in the number of unsatisfied bonds [19]. A newly bonded Ga atom makes two dangling bonds available for its adjacent As site with one coming from the new Ga atom, and the other from an existing (111)A sublattice Ga atom. The subsequent bonding of an As atom at that site can also take place with no change in the number of dangling bonds. This sequential nucleation of Ga and then the bonding of an As atom (i.e., lateral step growth) can be

similarly applied to (211)A epitaxial layer growth as well. The periodic step structure of (211) and (311) surfaces is expected to remain the same as the layer grows because the atomic arrangement of the growing surface should always be configured to minimize the number of dangling bonds.

4.2. Surface reaction mechanism in MBE growth

In molecular beam epitaxial growth, both the Group III and Group IV beam sources are normally atomic species with almost unity sticking coefficient [32], while the Group V and VI beam sources, which generally have relatively high vapor pressures and low sticking coefficients, are mainly molecular species [33]. In contrast to Si and Ge, C, which is a Group IV element, has an exceptionally low vapor pressure [32] so that in ordinary MBE growth C containing compounds, such as hydrocarbons, are the only effective doping sources for C acceptors [34]. In early surface studies of MBE growth mechanisms, it was found that the Ga adatoms can diffuse on the surface with a relatively long lifetime until they are either captured by As atoms and subsequently incorporated in the crystal or they evaporate. It has also been suggested that the incorporation of As from As_4 molecules, the dominant beam species when ordinary elemental As sources are used, involves several surface reaction processes. The physically adsorbed As_4, which is weakly bonded to the surface and thus mobile on the surface, can decompose into two As_2 molecules, either of which can be incorporated as a pair into two neighboring As sublattice sites [35,36]. The dissociative reaction rate of the diatomic As_2 depends on the available As site configurations [37]. Because of the relatively high desorption rate of As, the mean diffusion length of As_4 and As_2 admolecules is relatively small, and thus a stabilized As surface can only be obtained under conditions of high As_4/Ga ratios and relatively low substrate temperatures [38,39]. It can be assumed that the impurity adatoms of Group IV elements, Si and Ge, diffuse on the surface with fairly long lifetimes similarly to the Ga adatoms [29].

On (211)A and (311)A surfaces, a Ga adatom can easily diffuse on the surface and be trapped at the nearest step edge because the mean surface diffusion lengths are normally much larger than the step spacing. In addition, the physisorbed As_2 in the As stabilized condition, which implies large As_2 coverage on the surface, is immediately bonded to the Ga atoms at the step edge and thus incorporated on the As sublattice sites provided by the Ga atoms.

The As stabilized growth fronts on the (211)B and (311)B surfaces follow the same sequence as the (211)A and (311)A growth mechanism, with easy Ga nucleation and successive As bonding except that the Ga and As sites are interchanged in the bonding geometry. This continuous step edge growth, which is analogous to Frank's spiral growth [40] with an infinite radius, has been suggested to be ideal for perfect crystal growth [19].

Unlike the (211) and (311) polar surfaces, the (100) surface always has two double dangling bonds available for both Ga and As surface atoms so that mobile Ga adatoms can randombly bond to any Ga site [19] and then the As chemisorption can subsequently occur at the newly created sites under the As stabilized conditions. This random site incorporation of Ga can easily generate roughness of the (100) surface, and the Si and Ge impurity adatoms can randomly find the double bond sites as well. In spite of the random site growth of the (100) layer, two dimensional growth of the (100) orientation surface can be obtained by minimizing the statistical fluctuation [37] (or reducing the configuration entropy [41]) as long as the individual Ga adatom is extremely mobile and can cover a large surface area by surface diffusion [42].

In other studies of residual impurities in Si doped MBE GaAs grown on (100) substrates [43], we have found that a larger Ga surface diffusion coverage correlates with a reduction in the Si donor impurity incorporation. This supports the idea that a longer mean surface diffusion length for the mobile Ga adatoms on the (100) surface will provide a smoother surface with less impurity incorporation. However, the surface diffusion of Ga adatoms to the steps on the (211) and (311) polar surfaces is no longer the limiting factor in the growth process since the Ga surface diffusion length is sufficiently larger than the individual

step spacing of either (211) or (311) oriented surfaces. Consequently, all the step sites on the (211) and (311) surfaces can be reached effectively by the surface diffusion of mobile Ga adatoms during growth. Even if impurity adatoms arrive at the steps simultaneously with Ga adatoms, Ga adatoms preferentially incorporate at the step sites on (211) and (311) surfaces due to the nature of their different chemical bond strengths in GaAs growth. Thus the step growth can contribute to the suppression of the total Group IV concentration incorporated for MBE growth on (211) and (311) A and B surfaces respectively, relative to the total Group IV impurity concentration in (100) random site growth. However, the site preference of Group IV impurities on the polar surfaces can be enhanced over that on the (100) surface for the reasons given in the following discussion.

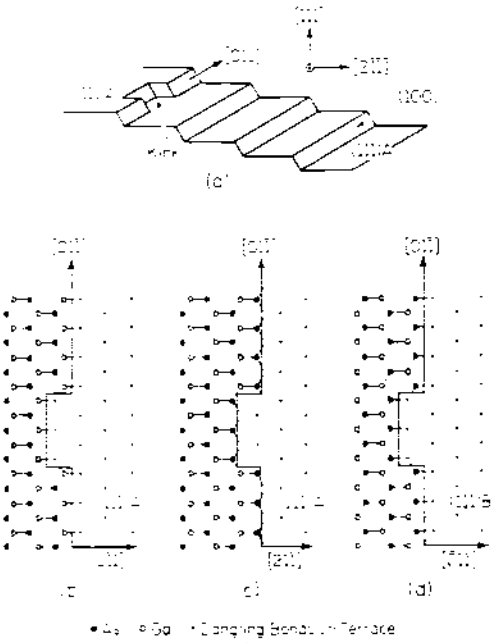

Fig. 4. (a) Schematic representation of the closed packed surface structure with periodic steps and kinks for (211)A or (311)A oriented surface. (b) Top view of the (211)A or (311)A surface structure with kinks in a step. (c) The same top view for (211)A or (311)A surface as (b) but showing an advance of uniform step edge by As bonding. (d) Top view of the (211)B or (311)B surface structure with kinks in a step.

4.3. Impurity surface reaction in MBE growth

Even though Group IV impurities can be strongly amphoteric due to random site selection on (100) oriented surface, Si incorporates preferentially as a donor in MBE (100) samples grown in the As stabilized condition. This high probability of Si impurities finding Ga sublattice sites is explained by the competition of Si impurity atoms with surface adsorbed Ga and As atoms [43]. In the As stabilized condition, defined by RHEED reconstruction pattern, although the true atomic nature of the surface structure has not been established, Si atoms can easily compete with Ga atoms for Ga sites which are randomly available through the surface diffusion, while they do not effectively compete with the abundant surface adsorbed As atoms for As sites.

On a (211)A or (311)A oriented surface, as a series of equidistant steps parallel to the [01$\bar{1}$] direction grow uniformly in the [2$\bar{1}\bar{1}$] direction, the individual step edge cannot be perfectly straight, but forms kinks. These kinks form because the surface diffusion of a Ga adatom toward a nearby step automatically creates kinks as shown in fig. 4a. The mobile adatoms of Si and Ge impurities can reach the step and join the As kink sites. From there it is very hard to escape since the bond energy of the As kink sites (3 dangling bonds) is much higher than on the step edge (2 dangling bonds) or flat (111)A terrace surface (1 dangling bond) as shown in fig. 4b [41]. This trapping growth mechanism at kinks can continue parallel to the [01$\bar{1}$] direction, generating a periodic bond chain (PBC). On the other hand, there is no particular Ga kink site with 3 dangling bonds on the A surface for easy trapping of the impurities as shown in fig. 4c which corresponds to monolayer growth on the surface in fig. 4b. The feather-like trace of the selectively trapped impurities at kinks was observed in LPE GaAs samples grown on substrates misoriented a few degrees from the (100) toward the (111)A orientation [44–46], and this suggests that two-dimensional layer growth on (100) surfaces is possible by the (111) step edge propagation with two ⟨110⟩ PBCs [47]. During the growth of the periodic bond chain parallel to the [01$\bar{1}$] direction on the (211)A and

(311)A surfaces, the incorporation of Si and Ge impurities is more probable on the As sites than on the Ga sites. This explains the fact that Si behaves preferentially as an acceptor for (211)A and (311)A oriented growth [13] and that the amphoteric ratio of Si is greater than 4 in MBE GaAs samples grown on (311)A substrates [20].

In contrast, it is the Ga kink sites on the (211)B and (311)B surface that have high bond energies and can easily trap a mobile adatom as shown in fig. 4d. A Ga adatom, which diffuses to a nearby step edge and incorporates there, creates a pair of As sites. These two adjacent As sites have the ideal configuration for the dissociative As incorporation of an As_2 molecule, leading to an increased incorporation rate for As. The relatively easy incorporation of Group IV impurity adatoms trapped at Ga kink sites and the efficient pairwise incorporation of As result in the preferential incorporation of Si as a donor in MBE growth on the (211)B and (311)B orientations. This explains that the site preference of Si for Ga sublattice sites in the (311)B layer is much greater than that in (100) grown layer.

Ge is more amphoteric than Si and incorporates preferentially as an acceptor under the growth conditions of the high substrate temperature and low V/III ratio in (100) MBE growth [48]. It was found that Ge is incorporated preferentially as a donor in MBE samples grown simultaneously on (100) and (311)B substrates at a V/III ratio of 20 and a substrate temperature of about 590°C. It was also shown that the amphoteric ratio of Ge ($[Ge_{As}]/[Ga_{Ga}]$) was 0.08 for the (311)B oriented sample and 0.37 for the (100) oriented sample [49]. This result indicates that the Ge amphoteric ratio is about 4 times higher than the Si amphoteric ratio for both (311)B and (100) oriented samples. however, the amphoteric behavior of Ge in the samples grown simultaneously on (311)A and (311)B substrates is similar to that of Si [20] due to the similar nature of the mobile Ge and Si adatoms.

Although the As kink sites have a higher bond energy for Si and Ge adatoms on the (311)A sites, these As kink sites, including As step edge sites, are not favorable for incorporation of C carried by hydrocarbons or other compounds that require a dissociative reaction process and removal of the foreign atoms or molecules before incorporation. This is because the foreign atoms or molecules attached to the C atom block the step propagation, thus inhibiting C incorporation until the foreign atoms or molecules are desorbed. This complicated dissociation process of the adsorbed C compound in MBE growth is analogous to that of the adsorbed GaCl molecules in VPE growth [50], which will be discussed in more detail in the following section. On the other hand, carbon is incorporated as an acceptor on the (311)B surface relatively more easily than on the (311)A surface since the foreign molecules of a C compound adsorbed at an As step edge site can be dissociated after a Ga adatom attaches to that C atom without hindrance of the step edge growth propagation in the $[2\bar{1}\bar{1}]$ direction [50]. With the surface reaction mechanism described above, the experimental orientation dependence of Group IV impurity incorporation in MBE growth summarized in table 2 can be understood [20,49].

Table 2
Orientation dependent incorporation of Group IV impurities in MBE growth

$[Si_{Ga}]_{(100)} > [Si_{Ga}]_{(311)B} > [Si_{Ga}]_{(311)A}$
$[Si_{As}]_{(311)A} > [Si_{As}]_{(100)} > [Si_{As}]_{(311)B}$
$[C_{As}]_{(100)} > [C_{As}]_{(311)B} > [C_{As}]_{(311)A}$
$[Ge_{Ga}]_{(100)} = [Ge_{Ga}]_{(311)B}$ [a]
$[Ge_{As}]_{(311)A} > [Ge_{As}]_{(100)} > [Ge_{As}]_{(311)B}$

[a] Because the amphoteric behavior of Ge is more dependent on growth conditions than that of Si, and because the donor and acceptor concentrations of Ge in the samples we studied are so small that quantitiave analysis of Ge is difficult, the experimental data for the orientation dependence of Ge incorporated on either (311)A and (100) orientations or (100) and (311)B orientations vary slightly between samples.

4.4. Surface reaction mechanism in VPE growth

In vapor phase growth, the Group III and IV sources are in the form of stable gaseous chloride compounds [15], while the Group VI impurity sources are in the form of the stable hydrides such as H_2S and H_2Se [52,53]. The hydride and chloride compounds of the Group V elements are thermally unstable and decompose to mainly poly-

meric compounds at the normal vapor growth temperatures [51]. Although the geometrical bonding structure in VPE growth is the same as in MBE growth, the surface reactions during growth and the impurity incorporation processes are expected to be quite different in VPE because of the different chemical nature of the source materials. The surface reactions of the Ga and As precursors at the substrate surface have not been observed directly, but the important role of the adsorbed GaCl, the main source of Ga in VPE, on the growing surface has been recognized based on the observation of different growth rates on different substrate orientations in $AsCl_3$-VPE [54,56]. Similar to the surface reaction behavior of mobile adatoms observed in MBE growth, the adsorbed molecules in vapor growth are essentially mobile, and diffuse toward the steps and perhaps also towards kinks [57]. There is little information about the geometrical structure of the adsorbed GaCl, though it can be postulated that the Ga atom from the GaCl admolecule binds to the surface, so that the Cl atoms can be dissociated from the admolecule by reacting with H_2 to form HCl gas, resulting in Ga incorporation in the crystal [54]. The removal of the Cl atom from the GaCl admolecule can occur either before or after an As atom bonds to the associated Ga atom. The particular bonding sequence that occurs depends on the substrate orientation.

In VPE growth on (111)B oriented substrates, the GaCl admolecules can diffuse and join the steps and kinks. These trapped GaCl admolecules interrupt the two-dimensional step propagation [50] through impurity poisoning of the step motion [58]. From fig. 4d, it is clear that the Cl atom bonded to Ga blocks the step growth since the adjacent As step site is not available for an incoming As atom until the Cl atom dissociates from the Ga–Cl admolecule [50]. As a result, As attachment at steps and kinks is extremely difficult, and consequently the step propagation is retarded. This qualitatively explains the observation that the lowest growth rate in $AsCl_3$-VPE growth occurs for the (111)B orientation [55]. A similar step poisoning effect has been observed in growth and etching studies of the ionic crystal LiF. It was found that a small concentration of FeF_3 in the solution, about 1 ppm, is enough to stop the growth of layers, because Fe ions occupy the step sites and kink sites which are more favorable, and inhibit the step growth [58–60].

On the other hand, Ga incorporation is very efficient at the steps on the (111)A surface [55] because the Cl atom of the Ga–Cl admolecule at the step or kink is positioned above the step and the incoming As atoms can easily attach to the Ga–Cl molecule forming an As–Ga–Cl admolecule [50]. As a result, the Cl atom can dissociate after the As atom bonds to the Ga–Cl molecule. This explains why the highest growth rate has been observed in the growth on (111)A substrates [55].

The reverse of this surface reaction mechanism has been observed in orientation dependent etching studies of Si using HCl vapor [61,62]. It was observed that the sites at the steps are more reactive than ordinary surface sites, and it was suggested that the surface diffusion of $SiCl_2$ admolecules is one of the important reaction processes. The vapor etching behavior of (100), (111)A, and (111)B GaAs substrates has also been studied using HCl vapor in a VPE reactor [63]. The orientation dependence of the etching rates was found to be similar to the orientation dependence of the growth rate. It was found that the etching rate of (111)A surface is higher that that of (111)B surface. It was observed by RHEED studies that the GaCl adsorption occurs only on (111)A surface, not on (111)B surface. These earlier results indicate that the incorporation reaction of Ga in the $AsCl_3$-VPE growth is not dependent on the surface diffusion of Ga adatoms, but it is dependent on the complicated reaction behavior of the Ga–Cl admolecules at surface.

4.5. Impurity surface reactions in VPE growth

The surface reaction behavior of chlorosilanes (SiH_nCl_{4-n}, where $n = 0$–4), which are the main form of the Si impurities in VPE reactors, is expected to be similar to that of GaCl. The molecular structure of chlorosilane vapor is known to have a tetrahedral bond geometry with a Si center atom, but the geometrical configuration of the molecular structure of chlorosilane after surface

adsorption of the Si atom is unknown. (See the tretment of adsorbed $GaCl_2$ [56].) The Si incorporation is assumed to be by reduction of the hydrogen chloride molecules from mobile chlorosilane (surface-Si–H_nCl_{4-n}) admolecules [61].

For VPE growth on (211)A oriented substrates, when the Si atom of a chlorosilane molecule ($Si–H_nCl_{4-n}$) occupies a Ga site on a (100) step edge, an As atom bonds to the adsorbed chlorosilane forming an $As–Si_{Ga}–H_nCl_{n-4}$ admolecule, which is the analogue to an adsorbed GaCl molecule on (111)A substrates. Eventually the remaining H_nCl_{4-n} molecule of the chlorosilane can dissociate from the Si_{Ga} atom which is strongly bonded to the three neighboring As atoms. When a chlorosilane molecule reaches the step edge on (211)A surface, its Si atom can join either an As step site or an As kink site. In either case, the H_nCl_{4-n} molecule blocks Ga atoms from bonding to the adjacent Ga site. Since the Ga site is blocked, the Si atom at the As step site is not firmly held and the whole chlorosilane molecule can be desorbed, while the Si atom at the As kink site is relatively firmly held but the chlorosilane interrupts the PBC growth. As a result, the amphoteric ratio of Si, $[Si_{As}]/[Si_{Ga}]$, is much lower in the (211)A VPE growth than in the (100) VPE growth, even though the total Si concentration ([Si]) in the (211)A layer is reduced substantially from that of the (100) layer. Similar incorporation behavior of Si for $AsCl_3$-VPE samples grown on (311)A surfaces is expected and has been reported [15]. The suppression of the Si acceptor in VPE (311)A growth and that the C acceptor in MBE (311)A growth can be explained similarly by the impurity poisoning effect at kinks, where the admolecules can neither escape nor incorporate easily as substitutional impurities. These trapped impurities can affect the step motion even when small concentrations are present [29,30,59].

The quantitative Si incorporation behavior as a donor in (211)B growth cannot be easily explained by the surface kinetic model discussed above since Ga step and kink sites are unfavorable for either Ga incorporation or Si donor incorporation. When the Si atom of a chlorosilane molecule occupies a Ga step or kink site, the admolecule blocks any As atoms from bonding to the adjacent As site. Thus the dissociation of the $Si–H_nCl_{4-n}$ molecule is necessary before the Si atom can bond to As and produce a Si donor. This is an analogue to the dissociative reaction process of an adsorbed GaCl on the same (211)B surface. As discussed earlier, this dissociation process contributes to the extreme difficulty of the Ga incorporation, resulting in the slow step propagation and the subsequently low growth rate on the (111)B and (211)B orientations. In a previous work, the Sn incorporation rate for intentionally Sn doped $AsCl_3$-VPE GaAs samples grown on (100), (111)A, and (111)B oriented substrates has been studied as a function of growth rate [16]. The result showed that the incorporation rate of Sn donors was substantially higher for (111) B layers than for both (100) and (111)A layers, and that the Sn donor concentration ($[Sn_{Ga}]$) in the (111)B layers was significantly increased with decreasing the growth rate. This relatively higher $[Sn_{Ga}]$ in the (111)B grown layers is consistent with the experimental result of the high Si donor incorporation behavior in (211)B and (311)B grown layers [15]. The explanation for this observed high Si donor incorporation rate in (211)B growth is that Si_{Ga} incorporation is enhanced presumably due to a relatively lower rate of dissociation reactions of the GaCl admolecules compared with the chlorosilane admolecules at steps and kinks.

Si impurities can also incorporate efficiently as acceptors on the (211)B surface. When the Si atom of a chlorosilane molecule occupies an As site, the foreign molecule H_nCl_{4-n} can dissociate after a Ga atom is added at the step, resulting in high Si acceptor incorporation. This incorporation reaction process for Si acceptors in (211)B growth is the same as that of Si donors in (211)A growth. As a result, the experimental orientation dependent Si incorporation observed in VPE growth [15],

$$[Si_{Ga}]_{(hh1)B} > [Si_{Ga}]_{(100)} > [Si_{Ga}]_{(hh1)A},$$

$$[Si_{As}]_{(hh1)B} > [Si_{As}]_{(100)} > [Si_{As}]_{(hh1)A},$$

where $h = 2, 3$, can be understood.

5. Summary and conclusions

In summary, three important experimental results have been observed in the Group IV impurity incorporation behavior. First, at fixed growth conditions (V/III ratio, source temperature, growth temperature, individual partial pressure of sources and impurities), the total impurity concentration and the amphoteric ratio of individual Group IV impurity species have been found to be strongly dependent on the substrate orientation. Second, although Si and Ge are generally similar in incorporation behavior, the orientation dependence of C incorporation is significantly different than that of Si in MBE GaAs; that is $[Si_{As}]_{(311)A} \gg [Si_{As}]_{(311)B}$ but $[C_{As}]_{(311)A} \ll [C_{As}]_{(311)B}$. Third, the Si amphoteric behavior in VPE (311)A layers is significantly different from that in MBE (311)A layers; that is, $[Si_{As}]/[Si_{Ga}] = 0.01$ in $AsCl_3$-VPE (311)A layers, but $[Si_{As}]/[Si_{Ga}] > 4$ in MBE (311)A layers.

These results clearly indicate that the incorporation and amphoteric behavior of Group IV impurities in epitaxial GaAs is kinetically influenced by the different surface reaction processes (adsorption, surface diffusion, dissociative chemisorption, and desorption) associated with the substrate orientation and the different chemical species for the two growth techniques. The growth on (211) and (311) oriented substrates has a (111) step growth component for two dimensional layer growth with step propagation in the $[2\bar{1}\bar{1}]$ direction and the growth of PBCs parallel to the $[01\bar{1}]$ direction in both VPE and MBE growth [29,55]. When the series of steps on the (211) and (311) surfaces are propagating, the impurities are easily trapped at continuously available kink sites. In the case of MBE growth, the mobile impurity adatoms of Si and Ge trapped at kink sites can easily be incorporated in the layer without affecting step motion. However, when the adsorbed C impurity compounds join kink sites, they cannot be easily incorporated as C_{As} but do interrupt the step motion through kink poisoning [30]. This kink poisoning effect can possibly alter the propagation direction of steps [29], and have an influence on impurity incorporation.

This interruption of step propagation is more obvious on the (211)B surface in VPE growth, because the GaCl admolecules require reduction of the chlorine before Ga incorporation so that they act as an impurity which reduces the step motion and growth rate. Even though the Ga step and kink sites are not favorable to either Ga–Cl or $Si–H_nCl_{4-n}$ molecules, the Si incorporation as a donor on the same growth orientation is enhanced presumably due to the relatively low dissociative chemisorption rate of GaCl. On the other hand, the Ga incorporation on (211)A becomes relatively effective and the Si_{Ga} incorporation on the same surface is minimized because there are no Ga kink sites but only Ga step edge sites, while the Si_{As} incorporation can be even lower due to the kink poisoning effect of adsorbed chlorosilane molecules at the As kinks.

In conclusion, the observed incorporation and amphoteric behavior of Group IV impurities for MBE and $AsCl_3$-VPE GaAs samples on polar orientations has been explained using different surface reaction processes and the bonding geometry on the different orientation. Although the impurity concentration in epitaxial layers is closely related to the partial vapor pressure of impurity sources over the substrate, we have demonstrated that the impurity concentration is kinetically reduced by increasing the effective surface reaction of Ga and As sources due to two dimensional step growth on (211) and (311) oriented substrates. The strong dependence of the Si amphoteric ratio on the epitaxial growth technique is due to the different reaction behaviors of the adsorbed chemical impurity species associated with the surface bonding structure of the dynamic growth front. This impurity reaction behavior is affected by the growth front dynamics, which are governed by the surface reactions of Ga and As source species. In contrast, the growth mechanism of the epitaxial process can also be affected by adsorbed impurities, which can geometrically alter the growth front by retarding the step motions by a poisoning effect. Therefore the impurity incorporation mechanism and the growth mechanism interact with each other and must be considered simultaneously. This explanation of the observed experimental impurity incorporation behavior, which is based on a combination of early experimental

results with our spectroscopic measurements and simplified assumptions discussed above, will hopefully provide additional clues that will lead to a full explanation of impurity incorporation and the epitaxial growth process.

Acknowledgements

This research was supported by the National Science Foundation under Grant NSF/DMR 83-16981 and by the Joint Services Electronics Program under Contract N00014-84-C-0149. The Center for Compound Semiconductor Microelectronics is supported by the National Science Foundation under Contract NSF/CDR 85-22666. We would like to thank B.L. Payne and R. MacFarlane for assistance in the preparation of this manuscript.

References

[1] T.S. Low, B.J. Skromme and G.E. Stillman, in: Proc. 10th Intern. Symp. on GaAs and Related Compounds, Albuquerque, NM, 1982, Inst. Phys. Conf. Ser. 65, Ed. G.E. Stillman (Inst. Phys., London–Bristol, 1983) p. 515.

[2] B.J. Skromme, T.S. Low and G.E. Stillman, in: Proc. 10th Intern. Symp. on GaAs and Related Compounds, Albuquerque, NM, 1982, Inst. Phys. Conf. Ser. 65, Ed. G.E. Stillman (Inst. Phys., London–Bristol, 1983) p. 485.

[3] C.E.C. Wood, J. Woodcock and J.J. Harris, in: Proc. 7th Intern. Symp. on GaAs and Related Compounds, St. Louis, MO, 1978, Inst. Phys. Conf. Ser. 45, Ed. C.M. Wolfe (Inst. Phys., London–Bristol, 1979) p. 28.

[4] G.M. Metze, R.A. Stall, C.E.C. Wood and L.F. Eastman, Appl. Phys. Letters 37 (1985) 165.

[5] P.D. Dapkus, H.M. Manasevit, K.L. Hess, T.S. Low and G.E. Stillman, J. Crystal Growth 55 (1981) 10.

[6] T.S. Low, M.H. Kim, B. Lee, B.J. Skromme, T.R. Lepkowski and G.E. Stillman, J. Electron. Mater. 14 (1985) 477.

[7] W.M. Theis, K.K. Bajaj, C.W. Litton and W.G. Spitzer, Appl. Phys. Letters 41 (1982) 70.

[8] S. Zemon, M.O. Vassell, G. Lambert and R.H. Bartram, J. Appl. Phys. 60 (1986) 4253.

[9] B.J. Skromme, S.S. Bose, B. Lee, T.S. Low, T.R. Lepkowski, R.Y. DeJule, G.E. Stillman and J.C.M. Hwang, J. Appl. Phys. 58 (1985) 4685.

[10] C.E.C. Wood, Appl. Phys. Letters 33 (1978) 770.

[11] D.J. Ashen, P.J. Dean, D.T.J. Hurle, J.B. Mullin, A.M. White and P.D. Greene, J. Phys. Chem. Solids 36 (1975) 1041.

[12] D.W. Shaw, in: Proc. 2nd Intern. Symp. on GaAs and Related Compounds, Dallas, TX, 1968, Inst. Phys. Conf. Ser. 7, Ed. H. Strack (Inst. Phys., London–Bristol, 1969) p. 50.

[13] W.I. Wang, E.E. Mendez, T.S. Kuan and L. Esaki, Appl. Phys. Letters 47 (1985) 826.

[14] B.H. Ahn, R.R. Shurtz and C.W. Trussell, J. Appl. Phys. 42 (1971) 4512.

[15] J.V. DiLorenzo, J. Crystal Growth 17 (1972) 189.

[16] C.M. Wolfe, G.E. Stillman and W.T. Lindley, in: Proc. 2nd Intern. Symp. on GaAs and Related Compounds, Dallas, TX, 1968, Inst. Phys. Conf. Ser. 7, Ed. H. Strack (Inst. Phys., London–Bristol, 1969) p. 43.

[17] T. Nakanisi, J. Crystal Growth 68 (1984) 282.

[18] S. Subbanna, H. Kroemer and J.L. Merz, J. Appl. Phys. 59 (1986) 488.

[19] R.C. Sangster, in: Compound Semiconductors, Vol. 1, Eds. R.K. Willardson and H.L. Goering (Reinhold, New York, 1962) p. 241.

[20] S.S. Bose, B. Lee, M.H. Kim, G.E. Stillman and W.I. Wang, J. Appl. Phys. 63 (1988) 743.

[21] P.C. Colter, D.C. Look and D.C. Reynolds, Appl. Phys. Letters 43 (1983) 282.

[22] G.E. Stillman, T.W. Low and B. Lee, Solid State Commun. 53 (1985) 1041.

[23] T.S. Low, B.J. Skromme, B. Lee, S.S. Bose, T.R. Lepkowski, N.C. Tien, G.E. Stillman and T.H. Miers, presented at Electronic Materials Conference in 1984, unpublished.

[24] I. Teramoto, J. Phys. Chem. Solids 33 (1972) 2089.

[25] D.T.J. Hurle, J. Phys. Chem. Solids 40 (1978) 647.

[26] H. Kunzel, A. Fisher and K. Ploog, Appl. Phys. 22 (1980) 23.

[27] R. Kaplan, Surface Sci. 116 (1982) 104.

[28] D.J. Chadi, Phys. Rev. B29 (1984) 785.

[29] H.C. Abbink, R.M. Broudy and G.P. McCarthy, J. Appl. Phys. 39 (1968) 4673.

[30] P. Hartman, in: Crystal Growth, Ed. P. Hartman (North-Holland, Amsterdam, 1973) p. 367.

[31] A. Kahn, Surface Sci. 168 (1986) 1.

[32] A.Y. Cho and M.B. Panish, J. Appl. Phys. 43 (1972) 5118.

[33] D.A. Andrews, R. Heckingbottom and G.E. Davies, J. Appl. Phys. 54 (1983) 4421.

[34] E.C. Larkins, E.S. Hellman, D.G. Schlom, J.S. Harris, Jr., M.H. Kim and G.E. Stillman, Appl. Phys. Letters 49 (1986) 391.

[35] J.R. Arthur, Surface Sci. 43 (1974) 449.

[36] C.T. Foxon and B.A. Joyce, Surface Sci. 50 (1975) 434.

[37] S.V. Ghaisas and A. Madhukar, J. Vacuum Sci. Technol. B3 (1985) 540.

[38] C.T. Foxon and B.A. Joyce, J. Crystal Growth 44 (1978) 75.

[39] J.H. Neave, B.A. Joyce and P.J. Dobson, Appl. Phys. A34 (1984) 179.

[40] F.C. Frank, Disc. Faraday Soc. 5 (1949) 48.

[41] P. Bennema and G.H. Gilmer, in: Crystal Growth, Ed. P. Hartman (North-Holland, Amsterdam 1973) p. 263.

[42] A. Madhukar and S.V. Ghaisas, Appl. Phys. Letters 47 (1985) 247.
[43] B. Lee, J. Szafranek, G.E. Stillman, K. Arai, Y. Nashimoto, K. Shimizu, N. Iwata and I. Sakuma, in: Frontiers of Surface Analysis, special issue of Surface and Interface Analysis, to be published.
[44] E. Bauser, M. Frik, K.S. Loechner, L. Schmidt and R. Ulrich, J. Crystal Growth 27 (1974) 148.
[45] E. Bauser and G.A. Rozgonyi, Appl. Phys. Letters 37 (1980) 1001.
[46] E. Bauser and G.A. Rozgonyi, J. Electrochem. Soc. 129 (1982) 1782.
[47] P. Hartman, Z. Krist. 119 (1963) 65.
[48] G.M. Metze, R.A. Stall, C.E.C. Wood and L.F. Eastman, Appl. Phys. Letters 37 (1980) 165.
[49] B. Lee, G.E. Stillman and W.I. Wang, unpublished.
[50] J.L. Larpote, M. Cadoret and R. Cadoret, J. Crystal Growth 50 (1980) 663.
[51] V.R. Ban, J. Crystal Growth 17 (1972) 19.
[52] J.V. DiLorenzo and G.E. Moore, Jr., J. Electrochem. Soc. 118 (1971) 1823.
[53] E. Veuhoff, M. Maier, K.H. Bachem and P. Balk, J. Crystal Growth 53 (1981) 598.
[54] D.W. Shaw, J. Crystal Growth 31 (1975) 130.
[55] J.B. Loyau, M. Oberlin, A. Oberlin, L. Hollan and R. Cadoret, J. Crystal Growth 29 (1975) 176.
[56] R. Cadoret, L. Hollan, J.B. Loyau, M. Oberlin and A. Oberlin, J. Crystal Growth 29 (1975) 187.
[57] W.K. Burton, N. Cabrera and F.C. Frank, Phil. Trans. Roy. Soc. London A243 (1951) 299.
[58] G.W. Sears, J. Chem. Phys. 33 (1960) 1068.
[59] G.W. Sears, in: Growth and Perfection of Crystals, Eds. P.H. Doremus, B.W. Roberts and D. Turnbull (Wiley, New York, 1958) p. 441.
[60] J.J. Gilman, W.G. Johnston and G.W. Sears, J. Appl. Phys. 29 (1958) 747.
[61] P. van der Putte, W.J.P. van Enckevort, L.J. Giling and J. Bloem, J. Crystal Growth 43 (1978) 659.
[62] P. van der Putte, L.J. Giling and J. Bloem, J. Crystal Growth 41 (1977) 133.
[63] M. Heyen and P. Balk, Crystal Growth 53 (1981) 558.